

2013

Pressure Signals in a Gas-Solid Fluidized Bed with Thermally Induced Inter-Particle Forces

Jaber Shabanian

Ecole Polytechnique de Montreal, Canada

Jamal Chaouki

Ecole Polytechnique de Montreal, Canada

Follow this and additional works at: http://dc.engconfintl.org/fluidization_xiv



Part of the [Chemical Engineering Commons](#)

Recommended Citation

Jaber Shabanian and Jamal Chaouki, "Pressure Signals in a Gas-Solid Fluidized Bed with Thermally Induced Inter-Particle Forces" in "The 14th International Conference on Fluidization – From Fundamentals to Products", J.A.M. Kuipers, Eindhoven University of Technology R.F. Mudde, Delft University of Technology J.R. van Ommen, Delft University of Technology N.G. Deen, Eindhoven University of Technology Eds, ECI Symposium Series, (2013). http://dc.engconfintl.org/fluidization_xiv/120

This Article is brought to you for free and open access by the Refereed Proceedings at ECI Digital Archives. It has been accepted for inclusion in The 14th International Conference on Fluidization – From Fundamentals to Products by an authorized administrator of ECI Digital Archives. For more information, please contact franco@bepress.com.

PRESSURE SIGNALS IN A GAS-SOLID FLUIDIZED BED WITH THERMALLY INDUCED INTER-PARTICLE FORCES

Jaber Shabanian, Jamal Chaouki*

Department of Chemical Engineering, Ecole Polytechnique de Montreal, Montreal, Quebec, Canada

* Corresponding author: Tel.: +1-514-340-4711 X 4034; fax: +1-514-340-4159.

E-mail address: jamal.chaouki@polymtl.ca.

ABSTRACT

In this work, the polymer coating approach was used to increase and control the level of cohesive interparticle forces (IPFs) in a gas-solid fluidized bed. In this method spherical inert particles are coated with polymer material with a low glass transition temperature in this method. Since the artificial IPFs are dependent on the temperature of the coated particles, they can be easily controlled by the temperature of the inlet air into the bed. To investigate the effect of IPFs on fluidization behavior, pressure signals were recorded at different bed temperatures, levels of IPFs, and superficial gas velocities, covering both bubbling and turbulent regimes.

INTRODUCTION

Particle size, shape, roughness, and density as well as interparticle forces are among the most important parameters affecting the behavior of powder materials. In regards to the significance of IPFs, there is no doubt that IPFs dominate the flow dynamics of Geldart's group C particles, which leads to a completely different behavior compared to the other groups of Geldart's classification with low or no IPFs. Also, research studies on the influence of temperature on fluidization have reported that some peculiar phenomena at high temperatures, such as the variations of the minimum fluidization velocity and voidage, the fixed bed voidage, the minimum bubbling velocity and voidage, the dense phase voidage, and the local two-phase flow structure, cannot be solely explained by modifying the properties of the fluidizing gas and the variation of the solid phase, interparticle forces, has to be taken into consideration, as well (1-4). Therefore, it is highly attractive to clearly address how IPFs can alter the hydrodynamics of a gas-solid fluidized bed.

Investigations into the effect of IPFs on the behavior of a gas-solid fluidized bed have been carried out using different approaches (5-10). Most importantly, however, unceremonious and accurate control of the level of IPFs to have a uniform adhesion throughout the particulate media is not an easy task. Among different methods and considering its valuable advantage, it was shown in previous work of our group (9) that the polymer coating approach is a superior methodology for investigating the influence of IPFs on the hydrodynamic behavior of a gas-solid fluidized bed. This method uses a spherical inert particle, which is coated with polymer material having a low glass transition temperature (9°C). Since the artificial IPFs are dependent on the temperature of the coated particles, they can be easily controlled by the temperature of the inlet air. Accordingly, the system temperature can be gently

varied near the glass transition temperature of the polymer, e.g., between 25 – 40 °C, to investigate the effect of IPFs on fluidization behavior. Interesting aspects of this method for increasing IPFs are uniform distribution of cohesion throughout the bed, simple and precise control of the level of adhesion by merely controlling the bed temperature, ability to work at low temperatures, and applicability of the technique for both low and high superficial gas velocities. More interestingly, this method is practical to reproduce and imitate the conditions found in fluidized beds operating at high temperatures in a friendlier environment in which unlike operating at extreme conditions, which is limited by the number of proper measurement techniques for hydrodynamic study, different measurement techniques can be easily used.

Since measuring pressure fluctuations together with different post-processing analyses on corresponding signals are relatively easy to perform, cost effective, nonintrusive, and applicable to a wide range of operating conditions and because pressure signals contain information about many phenomena that happen in a fluidized bed, such as bubble formation, coalescence, eruption, bed oscillation, etc., they have been broadly applied in fluidized bed research (11). In addition, to our knowledge, previous researchers collected the experimental data concerning for the effect of IPFs on the hydrodynamics of the bed at rather low gas velocities, often near the minimum fluidization/bubbling velocity, and there is no report at high gas velocities. For this reason, in the present work, nonintrusive pressure measurement was employed for investigating the influence of IPFs on the fluidization behavior of the gas-solid fluidized bed in bubbling and turbulent regimes. Through the post-processing of signals, the bed pressure drop, the standard deviations, and the Power Spectral Density (PSD) of time series of pressure fluctuations, at different operating temperatures and velocities are used to characterize the hydrodynamics of the bed under different conditions and, hence, brighten the impact of IPFs on the bed's behavior.

METHODOLOGY

The experimental work required first producing coated particles with a thin and uniform film of polymer on the surface of the base particles through an atomization process in a spheronizer. Afterwards, the coated particles were used in a gas-solid fluidized bed set-up and subjected to different temperatures by which IPFs changed.

Particle Coating Process

The first experimental step was to coat a thin and uniform polymer layer onto the surface of inert base particles. The polymer material employed for this purpose was a copolymer of Poly Methyl Methacrylate/Poly Ethyl Acrylate (PMMA/PEA) contained in a polymer suspension called Eudragit NE30D. A 450-720 μm cut of spherical sugar beads ($d_p=580\mu\text{m}$, $\rho_p=1556\text{ kg/m}^3$), which belongs to Geldart Group B particles and can accept a copolymer of PMMA/PEA as the coating, was chosen as the inert particles in this work.

The polymer suspension, which consists of a solution of copolymer PMMA/PEA in a 2 to 1 ratio, (Mass %: Water 70.0; PMMA/PEA 28.66; Nonoxynol100 1.33) was added by an atomization process onto the particles. The atomization process was achieved in a spheronizer in which the coated particles were simultaneously dried by heated air. More details about coating procedure and its operating conditions can be found elsewhere (9).

The characteristics of the final product are presented in Table 1. The thickness of the coating layer indicated in this table was evaluated by assuming an even distribution of polymer dry mass on all the particles while taking into account to the particle size distribution shown in Figure 1. It is worth mentioning that after coating process, variations in particle size and density for sugar beads were close to only 1% for both parameters, meaning a close similarity of the fresh and coated sugar beads from Geldart classification's point of view.

Table 1. Final Particles Coating Characteristics	
<i>Materials</i>	<i>Quantity</i>
Spherical sugar beads	3.0 (kg)
PMMA/PEA	0.10 (kg)
Mass percentage of coating	3.4 %
Coating layer thickness	$\sim 5 \mu\text{m}$

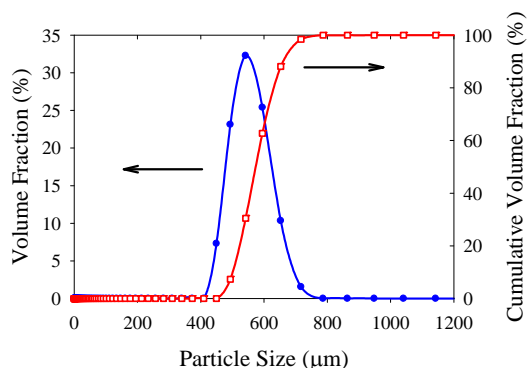


Figure 1. Particle size distribution of fresh sugar beads.

Experimental Set-up and Procedure for Fluidization Study

Experiments for the fluidization study were carried out in a gas-solid fluidized bed made of a transparent Plexiglas tube with a 15.2 cm inner diameter (I.D.) and 3.0 m in height. An external cyclone located at the air outlet of the column returned the entrained particles back into the freeboard of the bed. Dried and filtered air was injected into the bed through a perforated plate, as the distributor, with 157 holes 1 mm in diameter, arranged in 1 cm triangular pitch.

An electrical heater was used to heat up the fluidizing air before entering the fluidizing column. Accordingly, it was employed to adjust the temperature of the bed to a desired process setpoint. Temperature was controlled by means of a PI controller coupled with a thermocouple constantly immersed in the bed. The air flow rate was controlled with a calibrated rotameter, up to 0.65 m/s, and an orifice plate connected to a water manometer, at higher velocities. In this regard, different superficial gas velocities were used for each system and temperature tested, covering the fixed bed state, bubbling and turbulent regimes.

Uncoated/fresh and coated sugar beads, which were produced during the particle coating process, were separately used in the fluidizing apparatus at different operating temperatures to investigate the effect of IPFs on the fluidization behavior. Experiments of uncoated sugar beads were performed at 20°C whereas the ones for coated sugar beads were carried out at 20°C, 30°C, and 40°C. Hereafter, for the purpose of simplicity, we call these systems with their different operating conditions in abbreviated form, SB20, CSB20, CSB30 and CSB40, which stand for fresh sugar beads at 20°C and coated sugar beads at 20°C, 30°C and 40°C, respectively. When altering the temperature from one experiment to another, the flow rate of the air was readjusted according to the gas volume expansion and temperature in the bed to maintain the same superficial gas velocity at the bed temperature. It is worth emphasizing that variations in the air density and viscosity in the 20°C to 40°C temperature range are 6% and 5%, respectively, which are fairly insignificant compared to the degree of variation of cohesion, which rises from the polymer

coating approach for the same temperature range. All the experiments were conducted at ambient pressure. Also, the mass of particles introduced in the column for all experiments was 4.0 kg, which resulted in a static bed height of approximately 26 cm ($H/D \approx 1.70$) at ambient conditions.

In the present work, pressure fluctuations were measured with the use of sensitive pressure transducers connected to pressure probes equipped with in line 10 μm filters at their tip flush with the inner wall of the column. The pressure drop across the bed was measured using a differential pressure transducer while its legs were located at 0.95 cm and 2.0 m above the distributor. In addition, a gauge pressure transducer was employed to measure in-bed pressure signals. Since a gauge pressure transducer responds to every pressure fluctuation that occurs within the gas-solid bed (12), processing the time-series of the pressure signals obtained from the transducer gives a global view to what's happening inside the bed. The corresponding measuring probe was mounted on the column 17.5 cm in height above the distributor. This axial position for the pressure probe ensured it was far away from the turbulent effects of the distributor. The pressure data were recorded at a frequency of 400 Hz for a period of 240 seconds through a 16 bit A/D data acquisition board and with the help of the Labview 9.0.1® program.

Analysis Methods

The conventional method of bed pressure drop variation as a function of superficial gas velocity was used as the first indication of fluidization quality following the enhancement of IPFs in the bed and to evaluate the minimum fluidization velocity for different operating conditions.

Detailed information on the hydrodynamics of the bed can be obtained from scrutinizing the pressure fluctuations within the bed. These fluctuations normally originate from flow the of bubbles while other sources, such as formation, coalescence, and the eruption of bubbles, gas flow fluctuations, and bed mass oscillations, can also cause pressure waves in the bed (13,14). The two widely applied statistical properties of pressure fluctuations are the mean amplitude and power spectral density (PSD) of pressure fluctuations, which were evaluated in this study to obtain good information about the flow dynamics of the bed at different operating conditions. The mean amplitude of pressure data, which is generally expressed in the form of standard deviation and is a commonly used time domain analysis, can be calculated as the following:

$$\sigma = \sqrt{\frac{1}{N-1} \sum_{i=1}^N (P_i - \bar{P})^2} \quad (1)$$

where N is the number of data points at the sampling time interval and \bar{P} is the average of recorded P_i s. It is worth emphasizing that the standard deviation of the pressure fluctuation signals has an intense interrelation with mean bubble size.

The PSD of a signal, which is a frequency domain analysis, shows the contribution of every frequency in the spectrum to the power of the overall signal. It can be estimated from the magnitude of the square of Fourier transform of the signal. The variance of such estimation of PSD does not diminish with an increase in the number of data points. In order to decrease the variance, the signal is repeatedly divided into windows and an average of the PSD within the windows is applied to obtain an estimate for the PSD, which is actually the Welch method of PSD estimation. Hence, by choosing an appropriate window width to achieve a satisfactory trade-off between

frequency resolution and variance, the pressure signal was divided into L segments of distinct length of M. Accordingly, the PSD of each segment can be estimated by:

$$P_{yy}^i(f) = \frac{1}{\sum_{m=1}^M w^m(m)} \left[\sum_{m=1}^M P_i(m) w(m) e^{-j2\pi mf} \right]^2 \quad (2)$$

in which $P(m)$, $w(m)$, j , and f are the measured time series, window function, complex number, and frequency, respectively. Using Hanning window (w) and without any overlaps between windows, the average PSD becomes (15):

$$P_{yy}(f) = \frac{1}{L} \sum_{i=1}^L P_{yy}^i(f) \quad (3)$$

RESULTS AND DISCUSSION

The variation of the fixed bed height for uncoated and coated sugar beads is reported in Table 2. It shows that by increasing the level of cohesivity in the bed, the fixed bed height, and similarly the fixed bed voidage, increases. This indicates that a fixed particulate media with higher IPFs can hold more gas inside. In a similar manner, Formisani et al. (1) observed that voidage of the loosely settled bed of particles of Groups A and B increased with temperature. They attributed these findings to the increase of IPFs by temperature, which is supported by our results.

Table 2. Variation of Fixed Bed Height with IPFs

System	Fixed bed height (cm)
SB20	26.1
CSB20	27.2
CSB30	28.1
CSB40	30.2

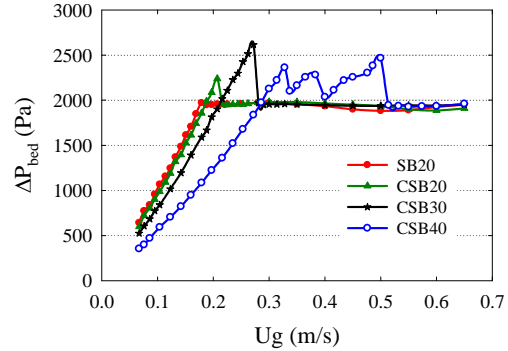


Figure 2. Effect of IPFs on the bed pressure drop profile in increasing the velocity path.

The variation of the whole bed pressure drop as a function of superficial gas velocity was used to give the first indication on how IPFs can alter the fluidization behavior. The bed pressure drop was first recorded while increasing the gas flow rate, and then while reducing the gas flow rate till all contents of the bed had settled down. Figure 2 shows the result of the measured pressure drop for beds with different levels of cohesivity while the gas velocity was increased (from a packed bed to a fluidized bed). It can be found that by enhancing IPFs (SB20, CSB20 and CSB30), the degree of overshooting in the “Increasing Velocity” curve increases, indicating a degree of powder cohesiveness, as is typical for group A powders. The fluidization of CSB40, which possessed the strongest IPFs inside, was characterized by the formation of cracks and rat holes at low velocities and lifting a portion of the bed as a plug rather than fluidizing it at moderate velocities. These are typical characteristics of group C materials. At higher velocities, due to the dominance of hydrodynamic forces (HDF) over IPFs, the whole bed became fully fluidized. These results show that an increase of cohesive IPFs can cause the behavior of the bed to change from Group B to Group A and even Group C powders. Additionally, Figure 2 shows that the minimum fluidization velocity (U_{mf}) increases when the role of IPFs is enhanced as a function of temperature.

Figures 3 and 4 show the pressure drop of studied systems during fluidization and defluidization branches. As can be found from these figures, the more the powder became cohesive, the larger the deviation between the curves of the pressure drop versus superficial gas velocity observed during increasing and decreasing fluidizing gas velocity. This observation is in accordance with experimental results of Lettieri et al (8), who investigated the effect of enhancing IPFs on the fluidization behavior of the Equilibrium FCC catalyst at high temperatures.

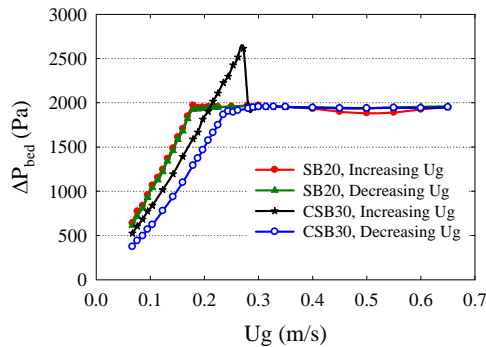


Figure 3. Bed pressure drop profile during increasing and decreasing velocity paths for SB20 and CSB30.

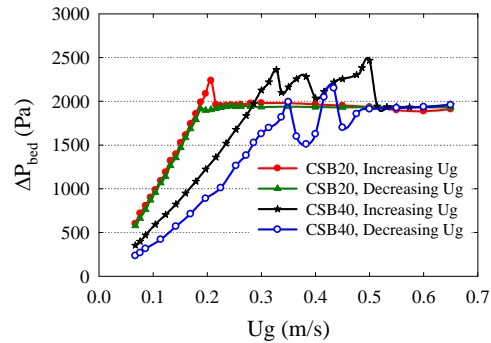


Figure 4. Bed pressure drop profile during increasing and decreasing velocity paths for CSB20 and CSB40.

The standard deviations of in-bed pressure fluctuations recorded by the gauge pressure transducer for different operating conditions are given in Figure 5. It shows that by increasing the superficial gas velocity for SB20, the standard deviation of pressure oscillations successively increased due to the increase in bubble formation and coalescence up to the critical U_c and then decreased with further increasing gas velocity since larger bubbles began to break up at velocities higher than U_c . According to Yerushalmi and Cankurt (16), the gas velocity at which the standard deviation reaches its peak is referred to as the transition velocity (U_c) from bubbling to turbulent regime. Inspecting Figure 5 at low velocities for coated sugar beads reveals that σ is lower for a system with stronger IPFs, at a constant superficial gas velocity. It can be regarded that the emulsion phase, in a similar manner to the fixed bed state, can hold more gas when the bed is more cohesive and, hence, at a constant gas velocity, smaller amount of gas is available to form bubbles. Accordingly, smaller bubbles are formed and weaker σ is obtained. However, the rate at which bubble size augments with fluidizing gas velocity increases with IPFs and curves of standard deviations for different systems cross each other at higher velocities in a bubbling regime resulting in higher σ for a more cohesive bed at velocities above 0.65 m/s. Another important observation is that dissimilar to SB20 for which U_c occurred at a specific velocity, transition from a bubbling to turbulent regime took place in a span of gas velocity for the bed with IPFs and it was expanded by enhancing cohesive forces. In other words, the cohesive bed shows resistance to the regime transition from bubbling to turbulent and this becomes more highlighted for a higher level of IPFs. Moreover, it can be found that enhancing IPFs in the bed, delayed the regime transition. These phenomena can be related to the reduction in the rate of bubble splitting considering the bubble splitting theory by the formation of particles of stalactite from its roof (17), due to the decrease in the fluidity of particles when the role of IPFs is enhanced.

The PSD resulting from the measurement of pressure oscillations inside the bed are plotted in Figures 6 – 8 for SB20 and CSB40. As can be found in these figures, at low

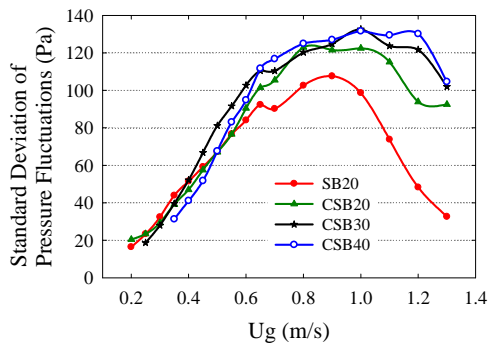


Figure 5. Standard deviation of pressure fluctuations from the gauge pressure transducer.

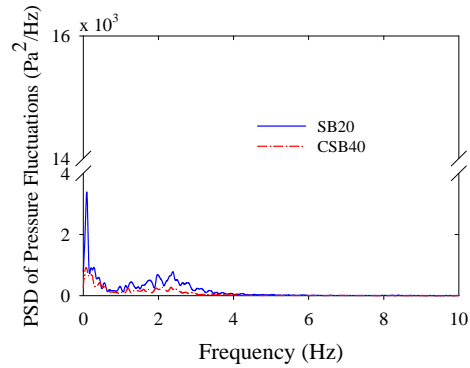


Figure 6. PSD of pressure signals from the gauge pressure transducer for SB20 and CSB40 ($U_g = 0.35$ m/s).

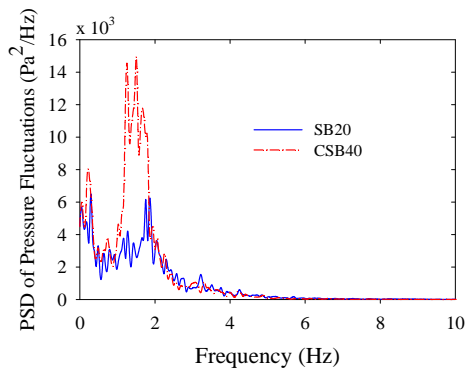


Figure 7. PSD of pressure signals from the gauge pressure transducer for SB20 and CSB40 ($U_g = 0.80$ m/s).

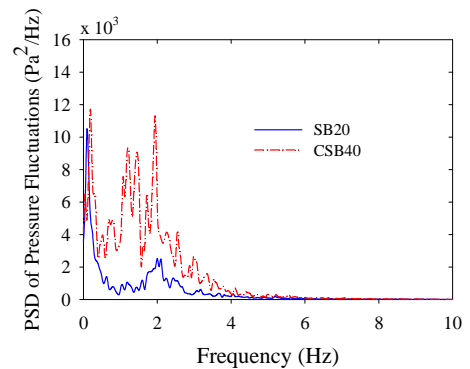


Figure 8. PSD of pressure signals from the gauge pressure transducer for SB20 and CSB40 ($U_g = 1.10$ m/s).

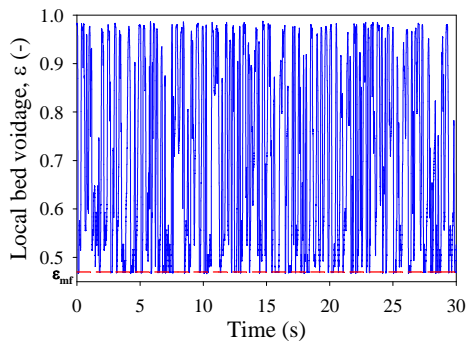


Figure 9. Signal of instantaneous local bed voidage for SB ($U_g = 0.40$ m/s).

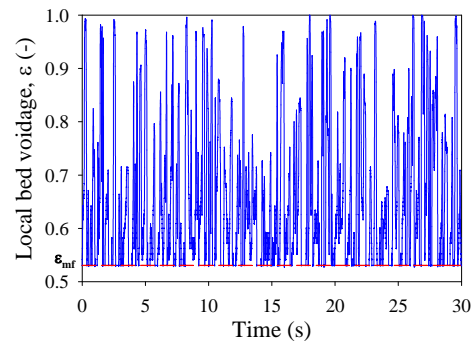


Figure 10. Signal of instantaneous local bed voidage for CSB40 ($U_g = 0.40$ m/s).

velocity, the peak corresponding to the dominant frequency for SB20 is more intense than for CSB40 confirming the presence of smaller bubbles for CSB40. Accordingly, for this condition while the two systems with different levels of cohesivity are compared to each other at the same superficial gas velocity, a more diluted emulsion phase and a higher tendency of the gas passing through the bed in the interstitial phase are expected for the bed with stronger IPFs inside. This was simply validated using the local bed voidage data obtained from an optical fiber probe immersed into the bed ($H = 20$ cm, $r/R = 0$) at different operating conditions. Figures 9 and 10 clearly exhibit that by intensifying IPFs the probe spends more time in the emulsion phase, which has a higher saturated emulsion value (ϵ_{mf}), rather than the bubble

phase and, hence, supports the experimental findings obtained from the pressure signals. By increasing the velocity, although the energy level of PSD increases for both cases, CSB40 holds a more intense peak at lower frequencies than SB20. This reveals that at high velocities, the more cohesive bed has bigger bubbles inside. These results are consistent with those obtained by analysis of standard deviation.

CONCLUSION

The analysis of experimental data obtained in this work indicates that the fluidization behavior of the particulate bed can shift from Group B to Group A or even Group C powders when the level of IPFs is enhanced in the bed. As far as the bed is fluidized, the bed with higher cohesivity shows milder fluidization with smaller bubbles at low gas velocities. However, bubble growth rate with superficial gas velocity is higher for the bed with stronger IPFs, which results in bigger bubble size at higher velocities of the bubbling regime. Also, it was noted that increasing IPFs postpones the regime transition from bubbling to turbulent while it is a perspicuous transition with respect to the gas velocity for a bed without IPFs. On the contrary, by increasing IPFs, the transition occurs slowly when the superficial gas velocity is increasing.

NOTATION

d_p	mean particle diameter (μm)	U_c	transition velocity form bubbling to turbulent (m/s)
f	frequency (Hz)	U_g	superficial gas velocity (m/s)
L	number of segments	U_{mf}	minimum fluidization velocity (m/s)
M	number of data points in each segment	ΔP_{bed}	measured pressure drop (Pa)
N	total number of data points		
\bar{P}	average pressure (Pa)	<i>Greek Letters</i>	
P_i	pressure signal (Pa)	ε	local bed voidage (-)
P_{yy}	averaged power spectral density (Pa^2/s)	ε_{mf}	minimum fluidization voidage (-)
$w(n)$	window function	ρ_p	particle density (kg/m^3)
P_{yy}^i	power spectral density for each segment (Pa^2/s)	σ	Standard Deviation (Pa)

REFERENCES

- Formisani, B., R. Girimonte, and L. Mancuso (1998). Chem. Eng. Sci. **53**(5): p. 951-961.
- Formisani, B., R. Girimonte, and G. Pataro (2002). Powder Technol. **125**(1): p. 28-38.
- Xie, H.Y., and D. Geldart (1995). Powder Technol. **82**(3): p. 269-277.
- Cui, H., and J. Chaouki (2004). Chem. Eng. Sci. **59**(16): p. 3413-3422.
- Geldart, D., N. Harnby, and A.C. Wong (1984). Powder Technol. **37**(1): p. 25-37.
- Seville, J.P.K., and R. Clift (1984). Powder Technol. **37**(1): p. 117-129.
- Rhodes, M.J., X.S. Wang, A.J. Forsyth, K.S. Gan, and S. Phadtajaphan (2001). Chem. Eng. Sci. **56**(18): p. 5429-5436.
- Lettieri, P., D. Newton, and J.G. Yates (2000). Powder Technol. **120**(1-2): p. 34-40.
- Shabanian, J., F. Fotovat, J. Bouffard, and J. Chaouki (2011). In T.M. Knowlton (eds.) CFB-10, 10th International Conference On Circulating Fluidized Beds And Fluidization Technology, Engineering Conferences International, New York: Sunriver Resort, Oregon, US.
- Bouffard, J., F. Bertrand, J. Chaouki, and S. Giasson (2012). AIChE J. **58**(12): p. 3685-3696.
- van Ommen, J.R., S. Sasic, J. van der Schaaf, F. Johnsson, and M.-O. Coppens (2011). Int. J. Multiphase Flow, **37**(5): p. 403-428.
- Davidson, J.F. (1991). AIChE Sym. Ser. **281**(87): p. 1-12.
- Tayebi, D., H.F. Svendsen, H.A. Jakobsen, and A. Grislingas (2001), Chem. Eng. Commun. **186**(1): p. 56 - 159.
- van der Schaaf, J., J.C. Schouten, F. Johnsson, and C.M. van den Bleek (2002). Int. J. Multiphase Flow, **28**(5): p. 865-880.
- Azizpour, H., R. Sotudeh-Gharebagh, R. Zarghami, and N. Mostoufi (2012). Particuology. **10**(3): p. 292-297.
- Yerushalmi, J. and N.T. Cankurt (1979). Powder Technol. **24**(2): p. 187-205.
- Clift, R. and J.R. Grace (1972). Chem. Eng. Sci. **27**(12): p. 2309-2310.